Available online at www.sciencedirect.com
SCIENCE DIRECT®
ELSEVIER
Solar Energy Materials & Solar Cells 88 (2005) 179–186
Solar Energy Materials & Solar Cells
www.elsevier.com/locate/solmat

Synthesis of black cobalt and tin oxide films by the sol–gel process: surface and optical properties

E. Barrera[a,*], L. Huerta[b], S. Muhl[b], A. Avila[c]

[a]*Departamento de Ingeniería de Procesos e Hidráulica, Universidad Autonoma Metropolitana—Iztapalapa, Av. Rafael Atlixco No. 186, Col. Vicentina, México D.F. 09340, México*
[b]*Instituto de Investigaciones en Materiales, UNAM, México D.F. 04510, México*
[c]*Sección de Electrónica del Estado Sólido, Depto. de Ingeniería Eléctrica, CINVESTAV, IPN, México*

Received 1 November 2003; received in revised form 1 February 2004; accepted 1 March 2004
Available online 18 January 2005

Abstract

Thin films of cobalt oxide (CO) and tin oxide (TO) were prepared by the dipping sol–gel method upon glass, stainless-steel (SS) and nickeled SS substrates. The aim of this study is to prepare selective photothermal coatings for medium temperature applications by superimposing TO films upon those of CO. Spectral reflectance measurements in both the UV–vis and the infrared ranges were used to characterize the relevant properties (absorptance and emittance). Also, atomic force microscopy and X-ray photoelectron spectroscopy (XPS) measurements were made on the films. The XPS data tells us that several phases of CO coexist (Co_3O_4, Co_2O_3) in the films under the preparation conditions used. Besides, large amounts of carbon were detected in several configurations: both as graphite particles and carbon bonded to metallic and oxygen atoms. Regarding the TO films, both SnO and SnO_2 phases were detected besides carbon particles as in CO. AFM studies made on samples upon glass substrates enable us to conclude that the dipping method yields surface morphologies with relatively low roughness, i.e., smooth film surfaces. By observing several tandem structures, it was found that placing a TO coating upon a CO film slightly improves the whole coating selectivity, but adding a nickel coating on the SS substrate improves even more such selectivity value.

Keywords: Black cobalt; Tin oxide; Sol–gel process

*Corresponding author. Tel.: +52 7 24 46 45; fax: +52 7 24 49 00.
E-mail address: ebc@xanum.uam.mx (E. Barrera).

0927-0248/$ - see front matter © 2004 Elsevier B.V. All rights reserved.
doi:10.1016/j.solmat.2004.03.010

1. Introduction

It is well known that efficient solar energy conversion requires selective absorber layers for the solar spectrum. The parameter representing the quality of the coatings for this purpose is selectivity, defined as the absorptance/emittance ratio (α/ε) [1–3]. A wide variety of techniques and coating materials have been used to obtain such selective coatings, however, the dipping sol–gel process has been less used for this purpose, probably because the thin film thickness is not enough [2,3]. However, the dipping sol–gel process for the preparation of thin films could offer the advantage of covering several kinds of substrates. For example, both glass and stainless-steel (SS) substrates are widely used in solar energy devices. Moreover, due to the relative simplicity of the dipping sol–gel method, low cost and ease of coating large surfaces, it results very attractive. The preparation of coatings by the dipping sol–gel process, has allowed us to make thin films with a uniform chemical composition because the technique is carried out in a uniform solution. Until now, there are previous studies concerning the independent cobalt oxide (CO) and tin oxide (TO) film preparation by the sol–gel process [3–5]. Moreover, due to its high chemical stability [5–7] we have formerly proposed the use of TO films to protect electrodeposited CO films [3]. In this work, we assess the selective performance of dipping sol–gel deposited TO films upon dipping sol–gel deposited CO films and the use of an electrodeposited nickel metallic substrate. Besides, we provide some information on composition of the above mentioned film materials.

2. Experimental

2.1. Sample preparation

Cleaning of the SS substrates consists of mechanical polishing and later rinsing in water. Then, substrates are kept in ethylic alcohol prior to the deposition; the glass substrates were rinsed in the same way and also kept in alcohol. Electrodeposited nickel coatings made by the typical Watts formulation [8] were deposited on steel substrates.

The precursor sols for CO films were prepared by a method similar to that used by El Bayadi et al. [9]. In our case, cobalt carbonate was precipitated by adding sodium carbonate to a starting aqueous cobalt nitrate solution (0.3 M). After rinsing and drying the precipitate was dissolved in propionic acid under strong stirring in order to form cobalt propionate (0.3 M). This product is used for the dipping processes. In this work, for the first CO layer three dipping–drying cycles of CO were applied to both SS and nickeled SS substrates. For tandem structures, the subsequent CO layers were made only with one dipping–drying cycle. In all cases, the drying temperature was 400 °C after each dipping.

2.2. Tin oxide deposition

The sol preparation was a modification of the Hiratzuka procedure [3], where a stannic chloride aqueous solution (0.1 M) is precipitated with sodium carbonate to

produce tin carbonate. After eliminating the excess salt by abundant rinsing, the precipitate was peptized in aqueous solution, obtaining a very stable tin sol (0.1 M). Tandem structures were fabricated upon both SS and nickeled SS substrates by depositing alternated CO and TO films.

2.3. Sample characterization

The solar absorptance was calculated from the spectral reflectance ρ_λ (in the wavelength range 0.20–2.5 μm) measured with a Varian Cary 5E spectrophotometer. Emittance was calculated by integration from near normal incidence reflectance measurements in the infrared range (2.5–25 μm) [10]. Measurements were made with a Nicolet 750 FTIR equipment (a gold mirror was used as a 100% reflectance reference).

The surface morphology of TO and CO films was studied with an AutoProbe CP Atomic Force Microscope from the Park Scientific Instruments company by using the contact mode. The RMS roughness was calculated from the experimental data. The film thickness was determined with a Dektak 2 profilometer.

X-ray photoelectron spectroscopy (XPS) was used to study the TO and CO films. The experimental setup was a VG Microtech MultilLab ESCA 2000 UHV system with a CLAM4 MCD analyzer and an Al Kα ($h\nu = 1486.6$ eV) X-ray source (operated at 15 kV and 20 mA). The incidence angle was 55° with respect to the surface normal and a constant pass energy $E_0 = 50$ eV was used. The VGX900 software was used to analyze the experimental results. The surface chemical composition was determined from the corresponding peak area by using the atomic sensitivity factor reported by Scofield [11] and corrected with the analyzer transmission function. The vacuum level during measurements was less than 1×10^{-9} mbar. The peak positions were refereed to the 1s carbon photo-peak at 274.5 eV. The FWHM was 1.4 eV referred to that from Ag $2p_{3/2}$.

3. Results and discussion

From thickness measurements, an average value of 128 nm was associated to each CO dipping–drying cycle. Then, an average thickness of 380 nm is assumed after three of such cycles upon either SS or nickeled SS. For TO films, an average thickness of 800 nm was determined for one dipping–drying cycle.

The surface morphology of the Co_3O_4 films is illustrated in Fig. 1, where one can see a very low roughness (RMS value = 47.1 Å). Moreover, from Table 1, the corresponding value for TO films is slightly lower. Hence, no texture-based radiation absorption trapping effect should be expected from coatings fabricated with these films.

The reflectance spectra of the (a) TO/CO/SS and (b) TO/CO/Ni/SS structures in the UV–visible range are shown in Fig. 2, while Fig. 3 depicts also reflectance spectra in the IR region for the same tandems.

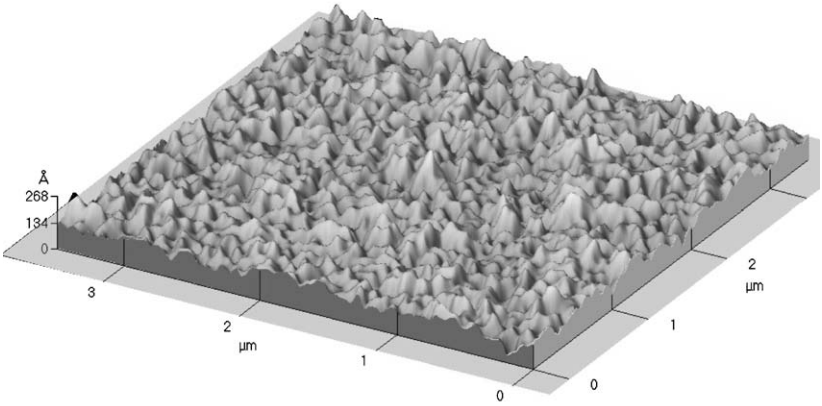

Fig. 1. Three-dimensional AFM view of the CO/SS surface morphology.

Table 1
RMS roughness of glass and several coatings prepared by the sol–gel method

Coating/surface	RMS roughness (Å)
Glass	6.18
TO	36.2
CO	41.7

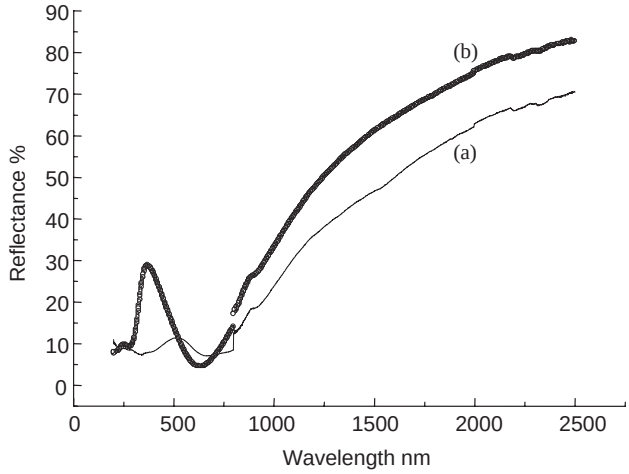

Fig. 2. Reflectance spectra in the UV-visible for (a) TO/CO/SS structure and (b) TO/CO/Ni/SS structure.

The absorptance and emittance constants were calculated according to the Duffie and Beckman methodology [10]. Despite, the absorptance constant is not high enough (see Table 2) the low emittance values allowed to calculate high selectivity

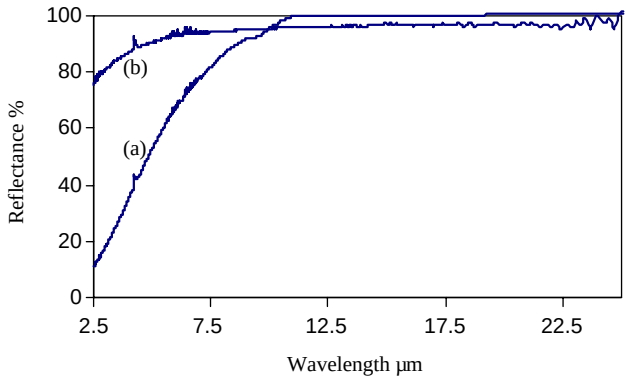

Fig. 3. Reflectance spectra in the infrared for (a) TO/CO/SS structure and (b) TO/CO/Ni/SS structure.

Table 2
Solar absorptance and emittance values at 100 °C and the resulting selectivity for several tandem structures on SS

Structure	α	ε	Selectivity, $s = \alpha/\varepsilon$
CO/SS	0.756	0.099	7.6
TO/CO/SS	0.782	0.088	8.8
TO/CO/Ni/SS	0.72	0.037	19.1
TO/CO/TO/CO/SS	0.784	0.087	9.0
TO/CO/TO/CO/Ni/SS	0.808	0.045	17.9

values (defined as the absorptance/emittance ratio) as shown also in Table 2. It is also clear that electro-depositing a previous nickel coating ($\cong 3\,\mu m$) upon the SS substrate, greatly improves selectivity. It should be noted that these improved selectivity values are even higher than those obtained for electrodeposited similar structures [3,4]. Increasing two layers, one of CO and one of TO, to the tandem does not seem to improve noticeably the absorptance and emittance constants, but adding the Ni layer at the bottom of the structure clearly does it.

3.1. XPS study

The surface composition of several tandems was studied by XPS measurements. Some of the peaks indicated in Table 3 were de-convoluted from the experimental signal of the samples shown in Fig. 4. Fig 4a depicts the de-convolution for the CO/SS tandem for the O 1s core level. Fig. 4b shows the de-convolution peaks for the same tandem, but for C 1s core level. Analogous to the tandem before, Fig. 4c and d show a similar case, but for a TO/CO/SS film.

It can be seen that the CO film is actually formed by two phases of CO, metallic cobalt and a large amount of carbon, which is most probably coming from the

Table 3
XPS quantitative results for typical samples after de-convolution

Sample	Spectral line	Atomic concentration[a] (%)	Formula	BE (eV)	Relative[b] (%)
CO/SS	O 1s	38.8	Co_3O_4	(529.60)	57.0
			Co_2O_3	(531.47)	28.2
			Fe_3O_4	(529.06)	14.8
	Co $2p_{3/2}$	17.9	Co_3O_4	(779.38)	85.5
			Co_2O_3	(781.57)	12.7
			Co_{metal}	(778.66)	1.8
	C 1s	43.3	C	285.73	83.8
			C/O/Co	287.27	16.2
SO/CO/TO/CO/SS	O 1s	22.3	SnO_2	(530.40)	83.6
			SnO, Co_3O_4	(529.29)	9.3
			O_{loss}	(535.87)	7.1
	Sn $2p_{3/2}$	8.4	SnO	(485.23)	54.5
			SnO_2	(486.12)	41.0
			[c]$Sn_{(complex)}$	(487.82)	4.5
	C 1s	67.2	C	285.66	79.4
			C/Sn/Co/O	287.54	20.6
	Co $2p_{3/2}$	2.2	Co_3O_4	(780.10)	88.5
			[c]$Co_{(complex)}$	(783.49)	11.5

[a]The uncertainty value estimated in area substraction, linear background and Scofield correction is 3%.
[b]The consideration of the errors associated with the analysis of elemental composition of surface coverage plus background and deconvolution peaks is estimated in 5%.
[c]Complex compounds (C, Cl, OH…).

precursor sol. The iron oxide fraction detected could probably correspond to some merging part of the substrate near the sample edges.

The TO film is also formed by two phases of TO, tin atom complexes, carbon particles and complexes. It can be seen that the spinel phase of CO and Co atom complexes are also observed. Again, this could be due to some merging part of the CO lower film near the sample edges or to the existence of pinholes in the upper film (TO). It is worthwhile to note that the phases coexisting (Co_2O_3 for CO and SnO for TO) with the main phase (Co_3O_4 for CO and SnO_2 for TO films), which was detected in XPS measurements for both films, has not been formerly detected by XRD measurements [3,4]. The surprising appearance of metallic particles should be further studied due to the advantageous effects of this cermet-like structure, which is also useful for selective surfaces [12].

4. Conclusions

Thin films of CO and TO grown by the dipping sol–gel method and tandem structures formed with these two components upon SS substrates, some of them with an electrodeposited Ni layer, were studied for solar selective absorption purposes. Quantitative analysis by XPS measurements made clear that the films contain more than one phase of the corresponding oxide, besides metallic particles and a great

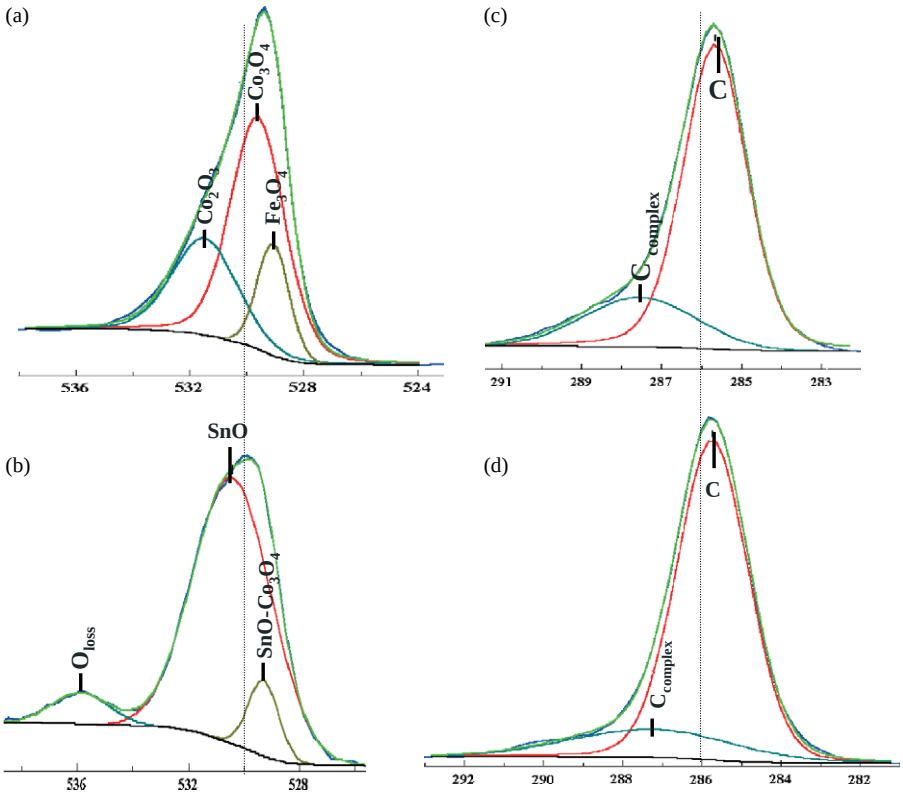

Fig. 4. The de-convolution XPS analysis of the O 1s and C 1s core level peaks for: (a) CO/SS structure for the O 1s core level, (b) CO/SS structure for the C 1s core level, (c) TO/CO/TO/CO/SS structure for the O 1s core level and (d) TO/CO/TO/CO/SS structure for the C 1s core level.

amount of carbon. This can be due to the relatively low annealing temperatures (400 °C) used in this work. The surfaces exhibit a smooth morphology with RMS roughness of 41.7 Å. Results on different tandem structures allow to conclude that inclusion of one or two TO/CO pairs does not change appreciably the total optical absorptance and emittance of the coating. Instead, inclusion of Ni layer below the TO/CO pairs greatly enhances such parameters, i.e., the best properties ($\alpha = 0.72$, $\varepsilon_{100} = 0.037$ therefore $s = 19.4$) were obtained for a coating having a structure TO/CO/Ni/SS. Further work on the films thickness control and also on the embedded metallic particle size should be later developed to optimize the important optical parameters.

Acknowledgments

This work was partially carried out with the financial support of CONACYT, projects 400200-5-36624-U and 39116 A. The authors thank José Guadalupe

Bañuelos Muñetón of CCADT, UNAM), for his assistance in the AFM characterization.

References

[1] C.G. Granqvist, Materials Science for Solar Energy Conversion System, Pergamon Press, Oxford, 1991.
[2] R.S. Hiratsuka, S.H. Pulcinelli, C.V. Santilli, J. Non-Cryst. Solids 121 (1990) 76.
[3] C.E. Barrera, G.T. Viveros, A. Montoya, M. Ruiz, Sol. Energy Mater. Sol. Cells 57 (1999) 127–140.
[4] E. Barrera, T. Viveros, A. Avila, P. Quintana, N. Batina, Thin Solid Films 346 (1999) 138–144.
[5] A.P. Rizzato, L. Broussous, C.V. Santilli, S.H. Pulcinelli, A.F. Craievich, J. Non-Cryst. Solids 284 (2001) 61–67.
[6] A. Maldonado, A. Tiburcio, R. Asomoza, Reporte Interno No. 53, CINVESTAV, IPN, México, 1993.
[7] C.J. Brinker, G.W. Sherer, Sol–Gel Science, Academic Press Inc., London, 1990.
[8] S. Pethkar, M.G. Takwale, C. Agashe, V.G. Bhide, Sol. Energy Mater. Solar Cells 31 (1993) 109–117.
[9] M. El Bayadi, S.K. Tiwari, R.N. Singh, J. Respringer, P. Chartier, J. Koening, G. Poillerat, J. Solid State Chem. 116 (1995) 157–169.
[10] J. Duffie, W.A. Beckman, Solar Engineering Thermal Energy Process, Wiley, New York, 1990.
[11] J.H. Scofield, J. Electron Spectrosc. 8 (1976) 129.
[12] C.S. Uma, L.K. Malhotra, K.L. Chopra, Thin Solid Film 147 (1987) 243–249.